Desalination and Water Treatment
www.deswater.com

doi: 10.5004/dwt.2021.27499

231 (2021) 348–358
August

Evaluation of orange peel (*Citrus sinensis*) as a source of bioactive components and its use as a bioadsorbent

José Alfredo Hernández Maldonado[a,*], Carolina Elizabeth Ceballos Aguilera[a], María Mercedes Salazar Hernández[b], Alba Nelly Ardila Arias[c], Rosa Hernández Soto[a]

[a]*Instituto Politécnico Nacional-UPIIG. Av. Mineral de Valenciana 200, Col. Fraccionamiento Industrial Puerto Interior, C.P. 36275 Silao de la Victoria, Gto, Mexico, Tel. +52 1 55 5729 6000 Ext. 81416; emails: jahmuam@gmail.com/ jahernandezma@ipn.mx (J.A.H. Maldonado), carolinaceballospa@gmail.com (C.E.C. Aguilera), rohernandezs@ipn.mx (R.H. Soto)*
[b]*Departamento de Ingeniería en Minas, Metalurgia y Geología, División de Ingenierías, Universidad de Guanajuato, Ex Hacienda de San Matías s/n. Fracc. San Javier, C.P. 36025, Guanajuato, Gto, Mexico, Tel. +52 473 732 22 91; email: merce@ugto.mx*
[c]*Facultad Ciencias Básicas, Sociales y Humanas, Politécnico Colombiano Jaime Isaza Cadavid. Carrera 48 N° 7-151 Bloque P19 Oficina 151, Medellín – Colombia, Tel. +57 4 319 7900 Ext. 483; email: anardila@elpoli.edu.mx*

Received 23 January 2021; Accepted 8 June 2021

ABSTRACT

The juices and nectars of orange produce large quantities of low-value commercial waste such as their peels. These residues have become a major environmental worry due to their high organic matter load, having a high fermentability rate, and causing serious economic and environmental problems for their disposal. However, these residues retain functional compounds such as vitamins C, phenols, and flavonoids which are recognized for their antioxidant, anti-inflammatory and anticancer properties. The present study aims to evaluate the Cr(III) adsorption capacity in aqueous solutions using treated orange peel (OPT) as adsorbent at 15°C, 30°C and 45°C and different ratios (8 to 40 g L^{-1}) of adsorbent-solution. The results show that the adsorption isotherms conform to the Sips model having the maximum adsorption capacity of 15.3 mg g^{-1} with 95% removal of Cr(III). It was observed that the process is endothermic and spontaneous. The adsorption kinetics of Cr(III) follows a pseudo-second-order model. Cr(III) removal using OPT was analyzed with the techniques of X-ray diffraction, Fourier-transform infrared spectroscopy, ultraviolet-visible and scanning electron microscopy images. The obtained results suggest that it is feasible to take advantage of OPT to obtain functional compounds and remove Cr(III) from aqueous solutions.

Keywords: Treated orange peel; Flavonoids; Bioadsorption; Cr; Isotherm; Kinetics; Removal

1. Introduction

Citrus cultivation in tropical and subtropical regions around the world is estimated at more than 100 million tons per season [1]. Among the main citrus fruits are oranges, tangerines, lemons, limes, grapefruit, etc., with orange being the most cultivated and commercialized citrus species in the world. Mexico is the fifth producer of orange worldwide [1,2]. Around 40% of the internationally produced oranges are used to make different commercial products, such as jams or fresh juices [3,4], large amounts of waste are generated during the industrialization of the orange, it is estimated that these wastes reach up 50% by weight concerning the benefited fruit. Orange peels contribute the most to the generation of solid waste [1,3,4].

* Corresponding author.

These residues are characterized by having a high polluting power as a result of their high moisture content (around 80%–90%) and fermentable sugars, low pH (3–4), and high content of organic matter (around 95% of total solids), causing serious economic and environmental problems for disposal [5]. Therefore, the elimination of orange residues, mainly fresh skins, has become a major problem for the citrus processing industries, in some cases the direct disposal of these wastes results in the contamination of large tracts of land, whose high content of residues in putrefaction presents a significant risk to local watercourses, affecting the natural and beneficial microbial flora of soils as well as the uncontrolled production of greenhouse gases [1,5,6]. Additionally, several studies have shown that orange peels have functional compounds such as fibers, organic acids, minerals, essential oils, flavonoids, and pectins [2,3,5,7,8], which are found in varying amounts depending on the fraction of the shell analyzed (Fig. 1), for example, the albedo is rich in cellulose, hemicellulose, pectin and phenolic compounds, while flavonoids, carotenoids and essential oils are concentrated in the flavedo [9,10]. Functional compounds can be used to produce products with added value, such as citric acid [8,11], oligosaccharide peptides [12], bio-flavorings [13], and bioethanol [14]. Flavonoids are widely used compounds in the food and pharmaceutical industries since they have a wide range of biological activities, among which are: antioxidant, antimicrobial, anti-inflammatory, antiviral, and prevention of coronary diseases and neurodegenerative disorders [3,7,15].

The extraction of flavonoids with organic solvents has been carried out from various natural sources such as wheat leaves, Siberian hawthorn, plants of Mosla Chinensis Maxim, Jiangxiangru and Simmondsia Chinensis [7,9,16–18], regarding the orange peel flavonoid extraction yields are about 5 to 12 g of flavonoids/kg of dry orange peel 11.36 ± 0.30 g routine equivalents per kg orange peel [2,9,10,19,20]. In the case of the orange peel, there is not enough data on the distribution of flavonoids in flavedo and albedo, which can hinder their integration as a factor in functional products [9,10,20]. Additionally, the extraction of flavonoids from oranges can be relatively simple, since these compounds are to a greater extent in the upper crust of the shell and only a small part in the inner part of the shell [3,7,9,19]. On the other hand, the search to abate the pollution generated by agro-industry waste has led to efforts to reduce and reuse the waste generated by it, specifically the husks of some citrus fruits to clean effluents containing dyes used in the textile industry and metals such as Cu, Mn, Co, etc. [4,21,22] which can cause various diseases in the lungs, nervous system and/or cancer among others [23,24], orange peel, in particular, has been used to remove dyes by obtaining coal from the shell [25,26], pesticides, and in the recovery of Mo(VI), among other elements [27]. The orange peel is a bioadsorbent with high availability, sustainability, renewability, non-toxic, low cost and it has been shown in several studies that it can have similar adsorption capacity compared to commercial adsorbents when its structure is chemically modified with organic and inorganic solvents [24,27–29], it has also been used for the removal of heavy metals such as Cd, Pb, Ni, Zn, Fe, and Cr [30–33] the latter even though it is an essential bio-element for the correct functioning of the metabolism in living beings, it can cause structural disturbances in the erythrocyte membranes or skin allergies when the concentration of Cr(III) is greater than 30 ppm, in addition, if found in rivers or lakes where the environment can actuate, it oxidizes to Cr(VI) causing severe damage to living things [7,27,34,35]. Industries such as metallurgy, electroplating, agrochemicals, leather tannery, among others produce large amounts of effluents that contain Cr [27,28,34], making bioadsorption treatment essential since it has proven to be one of the most efficient alternatives to remove heavy metals with Cr [36–39], the orange peel has been used with different pretreatments in the removal of these ions from aqueous effluents, showing encouraging results [39]. Based on this information the objective of this work is to evaluate the integral use of the orange peel for both obtaining functional compounds and in the adsorption of Cr(III) from contaminated water, analyzing the process at different temperatures and quantity of bioadsorbent.

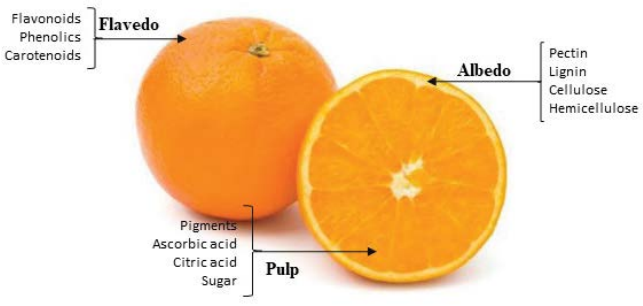

Fig. 1. Anatomy of the orange [3].

2. Methods and materials

2.1. Reagents

All the reagents used were of analytical grade. The solutions to be evaluated were prepared by dissolving chromium hydrated sulfate ($Cr_2(SO_4)_3{\cdot}xH_2O$) in deionized water, provided by Cuero Centro, S.A. de C.V., in concentrations of 300 mg L^{-1}.

2.2. Pretreatment of the orange peel

The orange peels were obtained from juice-producing micro-companies in the city of León, Guanajuato. Immediately after being harvested, the husks were rinsed with potable water, selecting for experimentation, the husks that did not show signs of decomposition as a change of coloration and bad smell. Manually, the residual pulp was removed from the shells. Afterwards, the husks were processed to obtain separately flavedo (F1), albedo (F2) and complete shell (F3), then the size of the material of the three fractions was manually reduced and dried with the help of a convection oven forced at 45°C for 72 h, once the drying time was finished, the dehydrated material was ground with the help of a ball mill (Gunt Hamburg CE 245), until obtaining particles with an average diameter of 250 mm.

2.3. Extraction of phenols and total flavonoids

For the extraction of phenolic and flavonoid compounds from the fractions F1, F2 and F3, the non-polar compounds were previously removed to avoid interference by maceration with hexane (HX) for 24 h. Once the maceration time had ended, the fractions were allowed to dry at room temperature. Subsequently, the three fractions were extracted with methanol (MT) using a ratio of 30% (p V^{-1}) at 35°C for 48 h, then the extracts were concentrated with the aid of a rotary evaporator (Büchi Labortechnik AG R II-HB) until the evaporation of the solvent is complete. The obtained extracts were stored for the determination of total phenols and total flavonoids in amber bottles at 4°C [40,41].

2.4. Analysis of total phenols

The quantification of total phenolic compounds was carried out by the Folin–Ciocalteu method, using the external calibration curve of gallic acid in concentrations of 0 to 1,000 mg L^{-1}. The absorbance was measured with a UV-Vis spectrophotometer (JENWAY 6507) at 760 nm. The concentration of total phenolic compounds was expressed as equivalent milligrams of gallic acid per gram of dry fraction [40,41].

2.5. Analysis of total flavonoids

For the quantification of total flavonoids, a calibration curve with serial dilutions of catechin (0.1 mg mL^{-1}) was used as standard. The absorbance of the samples at 510 nm was determined with the help of a UV-Vis spectrophotometer (JENWAY 6507), ensuring that the measurement will be made within a period of time less than 30 min after the end of the reaction [9,19,42,43].

2.6. Cr(III) adsorption isotherm

The tests of the adsorption isotherms of Cr(III) were carried out by adding a solution of 1 g of sorbent with 50 mL of Cr(III) to treated orange peel (OPT), in concentration between 0 to 200 mg L^{-1} in a shaker (ZHWY-200D) with 200 rpm agitation at 15°C, 30°C, 45°C for 24 h. After this time, an aliquot of sample was taken and then centrifuged (HERMLE Z383K) at 4,000 rpm for 10 min. Subsequently, the absorbance in the UV-Vis spectrum (JENWAY 6705) was measured at 425 nm, and the isotherm models used to describe the adsorption of Cr(III) with OPT were generated [43] and are shown in Table 1.

The amount of Cr(III) adsorbed in the analyzed material (q) [44]:

$$q = \frac{V\left(C_0 - C\right)}{m} \tag{1}$$

where C_0 is the initial concentration of the chromium solution and C is the concentration at time (t) in equilibrium (mg L^{-1}), V is the volume of solution (L) and m is the mass of OPT (g). In each case, the regression coefficient was calculated to evaluate the fit of each model using the SigmaPlot® software (Ver. 11) and the separation factor, R_L, in order to predict the affinity between the adsorbent and adsorbate [44]:

Table 1
Adsorption isotherm models [21,43]

Model	Equation
Sips	$q_e = \frac{q_m\left(K_s C_e\right)^{n_s}}{1+\left(K_s C_e\right)^{n_s}}$
Redlich–Peterson	$q_e = \frac{K_R C_e}{1+a_R C_e^{\beta}}$
Langmuir	$q_e = \frac{q_m K_L C_e}{1+K_L C_e}$
Temkin	$q_e = A + B\ln\left(C_e\right)$
Freundlich	$q_e = K_F C_e^{1/n}$

$$R_L = \frac{1}{1+K_L C_0} \tag{2}$$

where K_L is the constant of the Langmuir model (L mg^{-1}) and C_0 is the initial concentration of Cr(III). In order to determine the spontaneity of the adsorption process, the change in the apparent Gibbs free energy was calculated ΔG (kJ mol^{-1}) [45].

$$\Delta G = -RT\ln\left(55.5K_L\right) \tag{3}$$

and

$$k = 55.5K_L \tag{4}$$

where R is the ideal gas constant, T is the absolute temperature (K) and K_L is the constant of the Langmuir model. In addition, to determine the values of the enthalpy and entropy of the process:

$$\ln\left(k\right) = -\frac{\Delta H}{RT} + \frac{\Delta S}{R} \tag{5}$$

The values of ΔH and ΔS can be determined with the slope and classified according to the origin of the ln(k) graph as a function of T^{-1}.

2.7. Batch adsorption kinetics Cr(III)

The kinetics of Cr(III) bioadsorption were carried out in batches varying the concentration of OPT, from 8 to 40 g L^{-1}, at a speed of 200 rpm and temperatures of 30°C and 45°C, taking a sample volume every 90 min for 24 h. The samples were analyzed with the help of a UV-Vis spectrophotometer (JENWAY 6705). The kinetic models are shown in Table 2 [25,44]

Table 2
Kinetic models of adsorption [25,43,44]

Model	Equation
Pseudo-first-order (PFO)	$q = q_{\max}\left[1-\exp\left(-k_1 t\right)\right]$
Pseudo-second-order (PSO)	$q = \dfrac{t}{\dfrac{1}{k_2 q_{\max}^2}+\dfrac{t}{q_{\max}}}$
Elovich	$q = \dfrac{1}{\beta}\ln\left(\alpha\beta\right)+\dfrac{1}{\beta}\ln t$
Intraparticle diffusion (ID)	$q = k_{id} t^{0.5}$
External diffusion (ED)	$q = \dfrac{C_0 V}{m}\left[1-\exp\left(-k_{\exp} t\right)\right]$

The percentage of removal of Cr(III), $\%R_{Cr}$, was calculated [43].

$$\%R_{Cr} = \frac{\left(C_0 - C\right)}{C_0}\times 100 \tag{6}$$

In addition to using the coefficient of determination to compare the efficiency of the different kinetic and equilibrium models, the standard deviation, Δq, was calculated by Eq. (7) [43]:

$$\Delta q = 100\times\sqrt{\frac{\left(\dfrac{q_{\exp}-q_{cal}}{q_{\exp}}\right)^2}{N-1}} \tag{7}$$

where N is the number of data, $q_{\exp}$ and q_{cal} (mg g^{-1}) are the experimental and calculated values of the removed colorants, respectively.

2.8. Characterization of OPT before and after bioadsorption

The X-ray diffraction patterns (XRD) were obtained in a RIGAKU diffractometer (Ultima IV). The Fourier transform infrared analysis of the samples was performed in Perkin Elmer 100 Analyzer spectrophotometer in KBr pellets, using 32 scans and with a resolution of 4 cm^{-1}, in a range of 400–4,000 cm^{-1}. The scanning electron microscopy images and the X-ray energy dispersion spectroscopy (SEM-EDS-EDX) were obtained in a JOEL spectrometer (6510 pus). The adsorption spectra in the UV-Vis region were in a range of 1,100–200 nm.

3. Results and discussion

3.1. Content of phenols and total flavonoids

Table 3 concentrates the values obtained in the determinations of flavonoids and total phenols of the fractions analyzed. Regarding the content of total flavonoids in the F1 fraction the values obtained in the present study were higher than those reported by [45], who quantified 20.96 mg g^{-1} flavedo dry base, but lower than those determined by [10], who reported total flavonoid content of 29.74 mg hesperidin equivalents per g flavedo dry base. In contrast, the content of total flavonoids determined in F2 determined in the present work was lower than those reported for this same fraction by [10,45] who reported contents of 79.11 mg per g dry base albedo and 66.62 mg equivalent hesperidin per g dry base albedo, respectively. The reported differences can be attributed not only to the different extraction conditions applied by [10,45] (MT-DMSO, room temperature for 12 h but also to the disparity in the separation of the fractions, since in the three cases the separation of the shell in different fractions was done manually. According to the reported data, it is observed that high extraction temperatures applied in short times promote a greater extraction of flavonoids.

Table 3
Content of total phenols and flavonoids in the analyzed fractions

Fraction	Total phenols (mg AGE g^{-1})[a]	Flavonoids (mg QE g^{-1})[a]
F1	65.90 ± 6.5	27.75 ± 2.3
F2	40.50 ± 4.3	62.00 ± 6.2
F3	52.80 ± 6.0	46.20 ± 4.8

[a]Dry base

On the other hand, the content of total phenols determined in the fractions F1 and F2 obtained in the present study were superior to those reported by [10] who quantified 19.71 and 20.54 mg equivalents of gallic acid per g dry base fraction, which is probably due not only to the different extraction conditions used but also to the quantification methods applied. In contrast, [19] reported content of total phenols of 196.2 mg gallic acid equivalents per g dry base peel of the same orange variety, four times higher than that obtained in the present work and about 10 times more than the average value of orange peel obtained by [10]. There is high variability in the content of total phenols reported for orange peel (0.67–19.62 g/100 g dry base) [9]. In the case of F3, 46.2 mg g^{-1} of OPT was obtained when compared with that reported by [8], the amount of gallic acid obtained in this work exceeds 100 times that reported by the authors who used ethanol as an extracting solvent, this could be due to the variety of the fruit, the different state of the ripening stage, and even the region of its cultivation, the latter due to the regulation of gene expression and interaction with environmental factors, since, as it is known, phenolic compounds are secondary metabolites produced by the interaction with environmental factors such as climate, altitude, nutrition and agricultural practices [9].

3.2. Adsorption isotherms of Cr(III) with OPT

Fig. 2 shows the shape of the adsorption isotherms generated with the obtained data. The isotherms obtained independently of the temperature presented concave shape

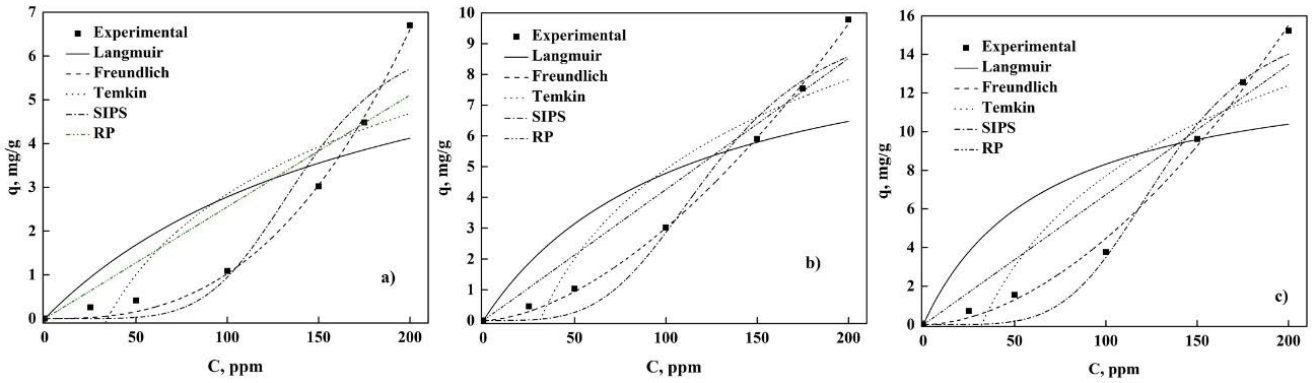

Fig. 2. Different isotherms for the bioadsorption of Cr with OPT: (a) 15°C, (b) 30°C and (c) 45°C.

downwards and the parameters obtained in the different models of isotherms is shown in Table 4.

According to the coefficient of determination (R^2) and normalized standard deviation (Δq), Sips (Table 4) was the most appropriate model for the description of the adsorption of Cr(III) in OPT, which suggests that adsorption occurs on the surface of the sorbent to reach a limit concentration, however, the values of $n_S > 1$ indicate that adsorption is due to the weak interaction (physical adsorption) between the orange peel and the Cr(III), which is reflected in the shape of the isotherm shown in Fig. 2. In contrast with the majority of adsorption studies made with orange peel, where isotherms of Langmuir or Sips type [26,29,43] have been obtained, indicating a favorable adsorption, the behavior obtained in the present study may be due to the characteristics of the used OPT, since the previous maceration with HX and MT eliminates various compounds of low polarity as essential oils, tocopherols, ascorbyl palmitate, and various free aglycones, which may influence the type of interactions between the surface of the OPT and Cr(III). The Freundlich model shows that the value of $1/n$ is between 1–10, which indicates that the adsorption process of Cr(III) on OPT is favorable [38].

Some authors have applied different treatments to orange peel, such as the use of formaldehyde and a contact time of 40 h, obtaining an adsorption capacity of 9.43 mg g^{-1} [46], other authors have used differently treated bioadsorbents for Cr(III) adsorption with which they obtained an adsorption capacity of 41.6 mg g^{-1} (EDTA-treated jackfruit), ground foxtail (11.7 mg g^{-1}) and *Sargassum filipendula* (33.02 mg g^{-1}) in all these works they found that the best-fitting model is the Langmuir model [26,29,47]. Other studies have observed that the best fit has been obtained with the Freundlich model using hydrotalcite [48] and *Nannochloris* microalgae [49] as adsorbent, obtaining an adsorption capacity of 17 and 34.7 mg g^{-1}. Comparing these results, we can mention that our adsorption of Cr(III) using OPT at 45°C is within the range of the capacity reported in the literature, having a removal percentage close to 95%, which allows us to consider OPT as a possible adsorbent. Table 5 shows the values of the thermodynamic properties of the adsorption process, which is carried out spontaneously ($\Delta G < 0$) and it has an increase in the adsorption capacity with the increasing temperature due to the endothermic nature of the process and the positive value of ΔS,

Table 4
Constant of the isotherm patterns in the adsorption of Cr(III) in OPT

Models	Parameter (GAC)		
	15°C	30°C	35°C
Langmuir			
K_L	0.0054	0.0092	0.0151
q_m	7.9540	10.057	13.827
R_L	0.481–0.882	0.352–0.813	0.248–0.725
R^2	0.6864	0.7452	0.6541
Δq, %	7.6409	1.1563	3.7364
Freundlich			
K_F	4.413×10^{-6}	0.0013	0.0011
n	0.3726	0.5959	0.5570
R^2	0.9940	0.9990	0.9856
Δq, %	0.4448	1.3822	0.9211
Temkin			
A	2.6566	4.1972	6.7517
B	0.0292	0.0323	0.0313
R^2	0.7565	0.8770	0.8556
Δq, %	23.695	22.6319	22.269
Sips			
K_s	0.0071	0.0079	0.0076
q_m	6.6821	10.051	15.102
n_S	5.2222	3.8673	4.6552
R^2	0.9961	0.9678	0.9956
Δq, %	0.1096	1.1312	0.3165
Redlich–Peterson			
K_R	2.9047	8.3759	6.3197
a_R	112.75	195.63	92.838
β	1.18×10^{-16}	1.18×10^{-17}	1.53×10^{-18}
R^2	0.8409	0.9439	0.9258
Δq, %	9.7053	5.2621	5.0765

Sips: K_s (L mg^{-1}), q_m (mg g^{-1}), n_S (adimensional); Langmuir: K_L (L mg^{-1}), q_m (mg g^{-1}), R_L (adimensional); Freundlich: K_F [(mg g^{-1}) (L mg^{-1})]$^{1/n}$, n (adimensional).

confirming that there is higher randomness between the OPT surface and the Cr [50].

3.3. Adsorption kinetics of Cr(III) with OPT

Based on the analysis performed at different temperatures and different kinetic models (Table 2) in the removal of Cr(III), it is feasible to know the cause that controls the process of adsorption which can be internal or external mass transfer, and the chemical reaction among others, and thus obtain a kinetic expression that allows describing the removal of Cr(III) from aqueous solutions at 30°C and 45°C. The models were applied to the experimental data, the parameters of the best models are shown in Table 6, where it is observed that the pseudo-first-order (PFO) and pseudo-second-order (PSO) models presented coefficients of determination of 0.99 and the normalized standard deviation (Δq) for both temperatures [43,44] the best fit was obtained with PFO model, which indicates that adsorption is fast under these conditions and that each ion of Cr(III) is linked with a OPT adsorption site [43,44]. The chemisorption energy of the Cr(III) ions increases as the concentration of adsorbent increases, since it directly increases the number of sites available for the process as the concentration of adsorbent in solution increases, similarly, to less amount of adsorbent, the smaller the number of sites available, being necessary greater adsorption energy to trap the Cr(III) ions [33]. Additionally, for both temperatures the models proposed to know the influence of the intraparticle diffusion and external transport, did not adjust appropriately to the experimental data, because it obtained a coefficient of determination lower than 0.1 and the normalized standard deviation was too high, which indicates that the process does not have mass transfer limitations [43].

On the other hand, the adsorption results of Cr(III) at 35°C (4.5 to 24.473 mg g^{-1}) and 45°C (4.99 to 31.33 mg g^{-1}) contrast with the low adsorption levels of Cr(III) in orange peel (8–20 mg g^{-1}) reported by [33,46] using orange peel treated with HCl and NaOH (11.67 mg g^{-1}) which could be explained based on the different treatments applied to the orange peel used, being the process applied in the present study very simple compared to those used by these authors. The literature has reported the use of various adsorbents obtaining different adsorption capacities for Cr(III) such as 35.2 mg g^{-1} [26] using yucca as adsorbent, 52 mg g^{-1} [51] using gelatin, and 6.58 mg g^{-1} [29] using ground foxtail as adsorbent. When using microorganisms as adsorbents, the adsorption capacity was 6.58 mg g^{-1} in the case of algae, 37.7 mg g^{-1} [49] in the case of *Nannochloris*, and 20.28 mg g^{-1} [47] in the case of *Sargassum filipendula*. Among these authors [30–33,47,51,52], were mentioned that the best models describing the adsorption kinetic process is that of PFO and PSO. Additionally, it was observed that the OPT used in the removal of Cr(III) from aqueous solutions presented better removal percentages compared to those

Table 5
Thermodynamic parameters of the adsorption process with OPT as a bioadsorbent

T, °C	$-\Delta G$, kJ mol^{-1}	ΔH, kJ mol^{-1}	ΔS, kJ mol^{-1} K^{-1}
15	23.13		
30	25.68	27.95	0.18
45	28.28		

Table 6
Parameters of the different kinetic models in the adsorption of Cr(III) in OPT

Model	Parameter	30°C					45°C				
		4 g L^{-1}	8 g L^{-1}	12 g L^{-1}	16 g L^{-1}	20 g L^{-1}	4 g L^{-1}	8 g L^{-1}	12 g L^{-1}	16 g L^{-1}	20 g L^{-1}
PFO	q_{max}	24.473	13.405	8.768	5.9028	4.5027	31.327	13.812	8.961	6.3445	4.9868
	k_1	1.898	1.3160	1.599	1.0449	0.9865	0.7292	2.1364	5154.2	158.65	1.9199
	R^2	0.9990	0.9950	0.996	0.9940	0.9950	0.976	0.9916	0.991	0.9760	0.9919
	Δq, %	1.3421	2.4561	1.7698	4.6843	4.3278	2.0215	1.0534	0.9756	0.8467	1.2145
PSO	q_{max}	24.285	13.136	8.9631	6.164	4.8083	34.077	13.7392	8.9699	6.3440	4.9891
	k_2	2.81×10^{-6}	1.48×10^{-6}	0.6850	0.4251	0.3954	0.0371	1.2×10^{-7}	8.9709	1.04×10^{6}	5.1228
	R^2	0.9996	0.9976	0.9961	0.9859	0.9999	0.9899	0.9959	0.9910	0.9764	0.9946
	Δq, %	0.8578	0.7354	0.5478	0.9762	0.9732	3.8623	1.9710	2.4378	3.8562	2.6401
Elovich	α	1.915	1.294	4.0534	2.999	2.3982	0.26384	0.2638	2.81×10^{6}	2.82×10^{6}	4.5595
	β	23.334	11.729	8.2101	5.1001	3.5787	22.511	22.511	9.9609	6.3440	4.6729
	R^2	0.9949	0.9930	0.9939	0.9709	0.9910	0.9897	0.9897	0.9910	0.9764	0.9980
	Δq, %	1.0045	2.8621	2.8452	1.9056	3.0231	5.0921	5.0921	2.5213	1.6457	1.7893
ID	k_{id}	21.034	43.345	48.094	37.092	25.764	11.101	25.345	30.492	9.0824	7.6004
	R^2	0.0985	0.0965	0.0905	0.0885	0.0801	0.0995	0.0811	0.0785	0.0787	0.0639
	Δq, %	65.342	45.342	85.342	65.342	65.342	35.344	28.142	40.249	35.092	61.009
ED	k_{ext}	0.0034	0.0014	0.0004	0.0009	0.0134	0.0074	0.0934	0.0544	0.0709	0.0211
	R^2	0.1059	0.0912	0.1085	0.0985	0.0935	0.0935	0.0995	0.0915	0.0898	0.1085
	Δq, %	55.042	35.421	25.291	45.152	15.029	23.102	25.981	41.099	33.307	48.945

obtained for Cr(III) with other agro-industrial residues (between 40% to 80%) such as pineapple, banana, potato, etc. [26,30–33,47,52].

3.4. Characterization of OPT

Fig. 3a and b show the XRD patterns of the OPT, before and after the adsorption process of the Cr(III) ions, in which the characteristic peaks of OPT are observed around 15° and 21° in both samples; which indicate that it is a highly ordered crystalline cellulose material, it is also possible to observe that the OPT material did not have significant deterioration either by the treatment with organic solvents or in the process of removal of Cr(III) ions, as reported in similar studies [43,53]. The presence of Cr(III) ions affects the intensity of some peaks present in the OPT at 30.7°, 36.0°, 38.2°, and 52.6°, which was also reported in studies carried out using Brushite as an adsorbent [43]. Using the Scherrer equation the crystal diameter was obtained for OPT (11.32 Å) and OPT-Cr (5.66 Å) observing a slight change due to the presence of Cr(III) ions in OPT, this same effect is observed with the lattice parameter decreasing from 4.744 Å to 4.65 Å, suggesting that a small Cr portion is introduced into the OPT structure in the process of removing the aqueous solution process waters.

On the other hand, Fig. 3c shows the infrared spectrum of the OPT before and after the adsorption process with Cr(III), where it can be seen that there are still functional groups in OPT interacting which interact with the Cr(III) ions [22,54,55]. In the case of OPT and based on the vibrations reported in the literature [56], the peak located at 3,343 cm^{-1} is due to the interaction of the OH groups of pectinic acid, hemicellulose and water absorbed by the pretreated shell. The peak located at 2,927 cm^{-1} corresponds to the stretching vibration of the C–H to CH_2– groups while the signal at 1,434 cm^{-1} is due to the symmetric movements of stretching COO^- and to the bending vibrations of the aliphatic groups. The band at 1635 cm^{-1} is attributed to the movement of the aromatic carbonyl and the carboxyl groups [22,54,55], while the band observed at 1,277 cm^{-1} is attributed to the presence of the stretching of the C–H bond of the phenol groups. Around 1,040 cm^{-1} it is observed

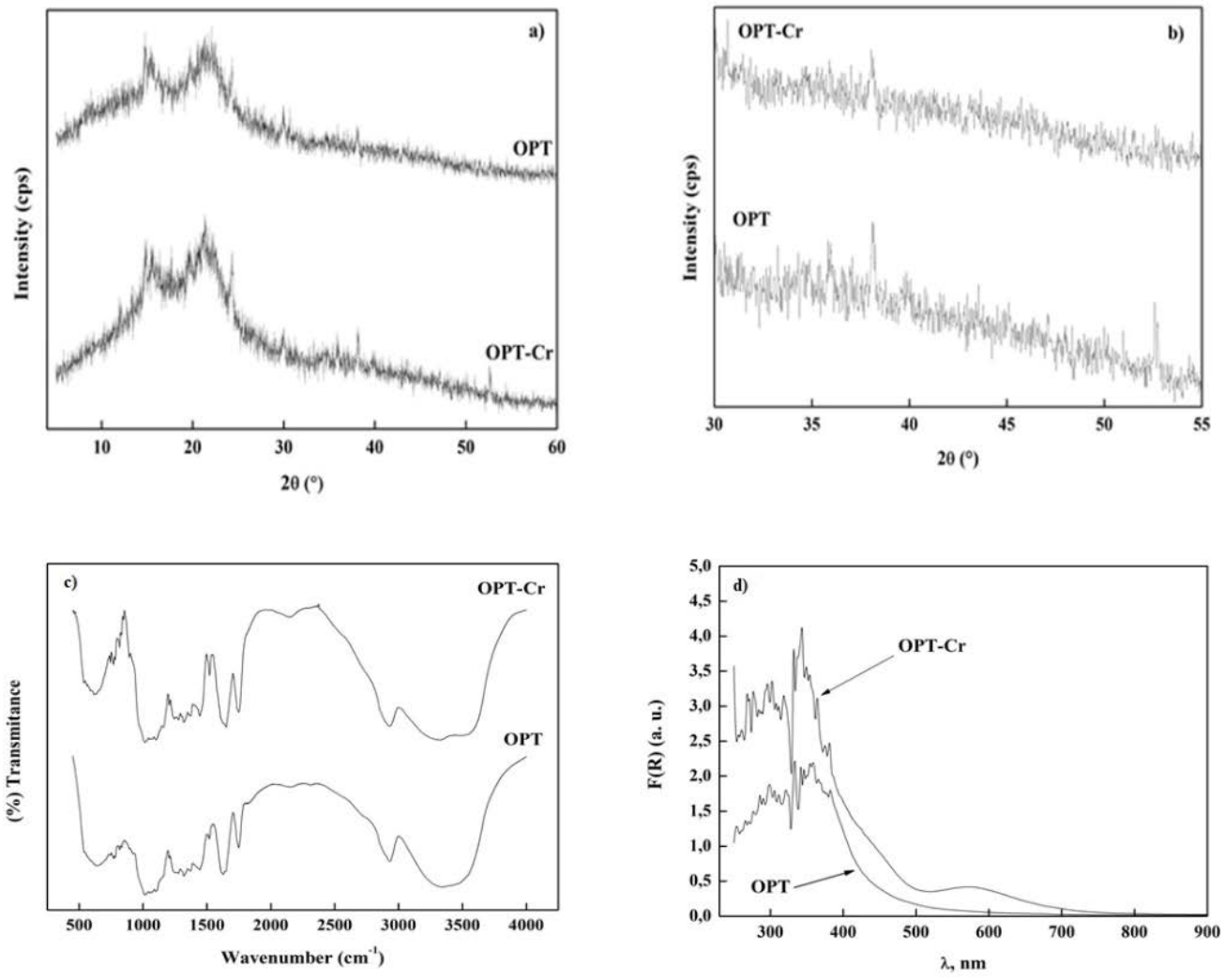

Fig. 3. Characterization of OPT before and after the removal of Cr(III).

a set of overlapping bands which are due to the presence of the vibrations of the C–O bonds of the primary and secondary hydroxyl and the carboxylic acid [22,53–56].

Once the process of removing Cr(III) from the OPT was carried out, significant changes were observed in the infrared spectrum of the sample (Fig. 3c). In the zone of the O–H vibrations, the formation of two bands is observed, at 3,510 and 3,300 cm^{-1}, it is also observed that the band and shoulder present at 2,937 and 2,847 cm^{-1} respectively, show a decrease in their intensity concerning the OPT before the process of adsorption and desorption of chromium, which is probably due to changes in the properties of the methyl groups; additionally, the peaks at 1,756 and 1,648 cm^{-1} present an increase in intensity which implies that carboxylic acid and carboxyl groups are affected, suggesting that these species may be directly related to the adsorption of Cr(III) on OPT [22,54,55,56].

Fig. 3d shows the UV-Visible spectrum for OPT doped with Cr(III) before adsorption, where it is observed that in the charge transfer zone (between 200 to 400 nm) of the OPT spectrum suffers an intensity change due to the presence of Cr(III) ions. On the other hand, in the spectrum of shell doped with Cr(III) a band around 580 nm is observed, which is directly related to the presence of Cr(III) in OPT, which agrees with what was observed in IR spectra, where some peaks assigned to groups that are on the surface of orange peel are affected by the presence of Cr(III) [22,54,55].

Fig. 4a and b show the micrographs taken at OPT, where several zones derived from the different species remaining on the surface of the adsorbent are observed as remnants of the pretreatment with applied organic solvents. Fig. 4c and d show that the surface does not undergo major modifications due to the presence of Cr(III) ions, however it is observed that there is formation of "clusters" in the OPT cavities [43,46,57], which are responsible for the changes seen in the IR and UV-Vis spectra. The elemental analysis (EDS) of the sample of OPT doped with Cr(III), where there were found characteristic elements of the groups present on the surface of OPT such as oxygen, carbon, silicon, phosphorus, calcium and others were found, the presence of Cr(III) was also detected, which confirms the removal of this metal with OPT [43,46,57]. Based on these results, we can infer that OPT is a good candidate for the creation of biofilters that can be used in contaminated effluents for the removal of Cr(III).

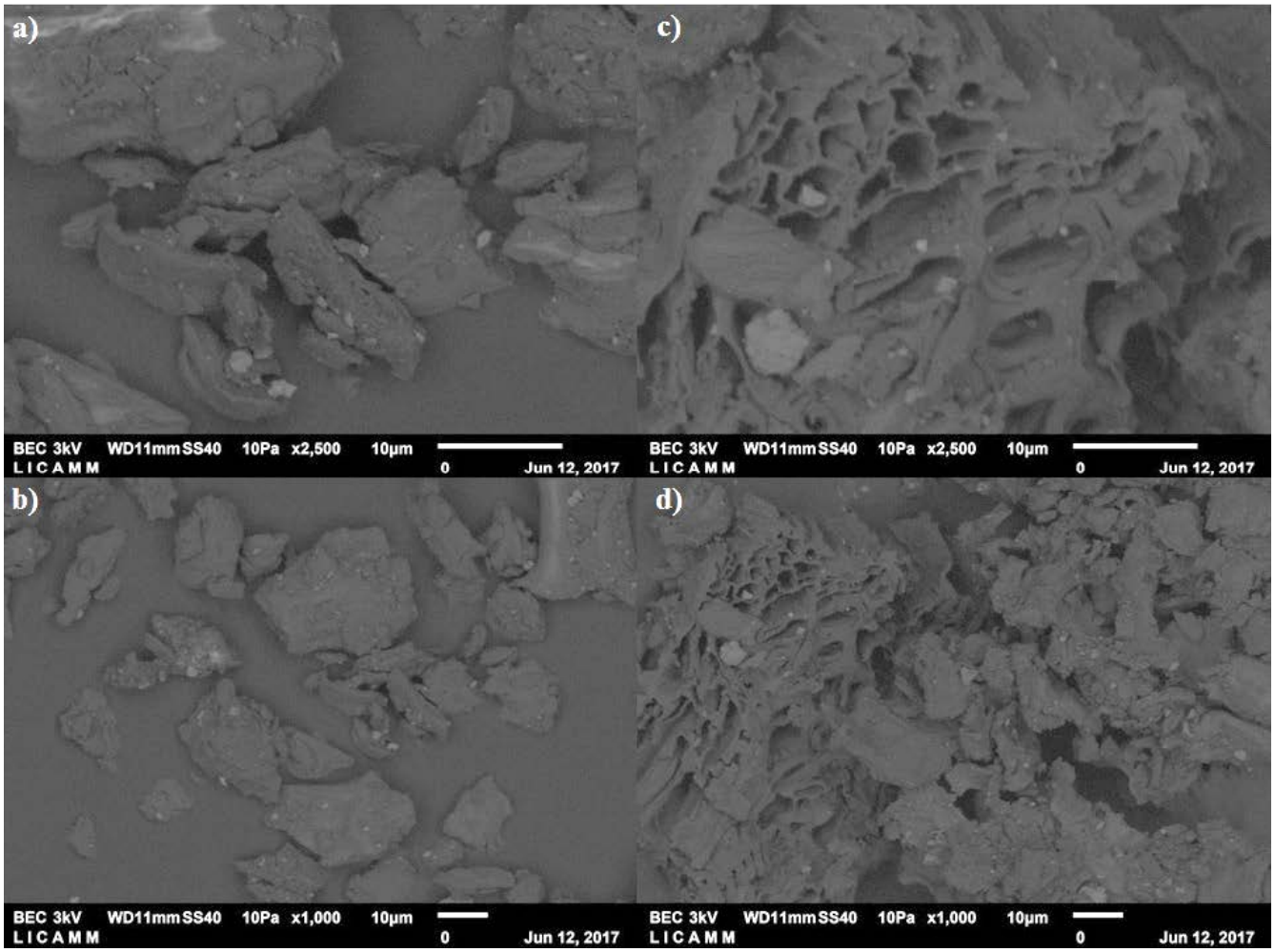

Fig. 4. Crystallographic images (a, b) OPT and (c, d) OPT-Cr.

4. Conclusion

The results obtained show that the treated orange peel (OPT) has a high removal of Cr(III) in aqueous solutions from a temperature of 15°C, 30°C and 45°C (close to 96%). The thermodynamic parameters of the adsorption process indicate that it is of endothermic nature and spontaneous, whence the adsorption capacity increases with increasing temperature. The removal of ions is carried out on the surface in more than one layer reflecting that the process is favorable ($1/n$ between 1 and 10). The kinetics of Cr removal was observed that the best fit is with the PFO model which indicates that each active site on the surface is used for the adsorption of the metal ions, moreover the value of the adsorption capacity reveals that it has a good adsorption when compared with other works so it can be considered that OPT is a candidate to be used in the removal of Cr(III) from aqueous solutions. XRD analysis showed that changes occur in the lattice parameter of OPT, indicating that there is Cr ion cluster within the crystalline structure of OPT, this was confirmed by SEM images showing Cr clusters in the surface cavities of the adsorbent and UV-Vis spectra of the samples before and after the process showing the presence of Cr(III) surface plasmon on the bioadsorbente. The FTIR study performed on the bioadsorbent shows the presence of several characteristic functional groups of OPT as OH, methyl, carboxyl, aliphatic groups, among others, that after adsorption of Cr(III) on the surface undergo changes, which leads to the conclusion that there is active participation of the OPT surface in the capture of metal ions.

Author´s contributions

JAH: Experimental analysis and drafting of the manuscript; CECA: Carrying out experiments; MSH: Analysis of the characterization of the samples; ANAA: Performing OPT Characterization; RHS: Analysis of OPT compounds and drafting the manuscript. All authors contributed to the research article and approved the final version.

Funding

The author's would like to thank the Research and Postgraduate Secretariat for the financial support for this work (SIP: 20160593) and to the BIOCATEM Network.

Acknowledgement

All authors would like to thank the Mining, Metallurgy and Geology Engineering Department of Guanajuato University and UPIIG-IPN for the infrastructure provided to carry out this project; and we also thank to engineers Laura Patiño Saldivar, Samuel Marias Burgos and Luz Gabriela Orozco Guerra.

Symbols

m	—	Mass of nDCPD, g
V	—	Solution volume, L
C_0	—	Cr(III) concentration initial, mg L^{-1}
q	—	Adsorption capacity of Cr(III) with the solid phase, mg g^{-1}
q_m	—	Maximum adsorption capacity of Cr(III) ions, mg g^{-1}
ΔG	—	Gibbs free energy, kJ mol^{-1}
ΔH	—	Enthalpy, kJ mol^{-1}
ΔS	—	Entropy, kJ mol^{-1} K^{-1}
R	—	Ideal gases constant
T	—	Absolute temperature, K
K_L	—	Langmuir model constant, L mg^{-1}
R_L	—	The regression coefficient, dimensionless
K_s	—	Sips constant related to energy adsorption, L mg^{-1}
n_S	—	Sips model dimensionless parameter, dimensionless
K_R	—	Redlich–Peterson constants, L mg^{-1}
a_R	—	Redlich–Peterson constants, L $mg^{-1\beta}$
β	—	Exponent ($0 < \beta < 1$), dimensionless
A	—	Temkin model constants, L mg^{-1}
B	—	Temkin model constants, kJ mol^{-1}
K_F	—	The Freundlich model constant of related to the adsorption capacity $[(mg\ g^{-1})(L\ mg^{-1})]^{1/n}$
$1/n$	—	The adsorption reaction energy, dimensionless
k_1	—	Kinetic constant de PFO, h^{-1}
k_2	—	Kinetic constant de PSO, g mg^{-1} h^{-1}
α	—	Initial adsorption rate, mg g^{-1} h^{-1}
β	—	Relationship of the surface area covered and the activation energy by chemisorption, g mg^{-1}
q_{exp}	—	Experimental value of Cr(III) ions adsorbed in equilibrium, mg g^{-1}
q_{cal}	—	Calculated value of Cr(III) ions adsorbed in equilibrium, mg g^{-1}
N	—	Number of data
$\%R_{Cr}$	—	Cr(III) removal percentage

References

[1] A.S. Matharu, E.M. de Melo, J.A. Houghton, Opportunity for high value-added chemicals from food supply chain wastes, Bioresour. Technol., 215 (2016) 123–130.
[2] K. Sharma, N. Mahato, M.H. Cho, Y.R. Lee, Converting citrus wastes into value-added products: economic and environmently friendly approaches, Nutrition, 34 (2017) 29–46.
[3] S. Rafiq, R. Kaul, S.A. Sofi, N. Bashir, F. Nazir, G.A. Nayik, Citrus peel as a source of functional ingredient: a review, J. Saudi Soc. Agric. Sci., 17 (2018) 351–358.
[4] I. Anastopoulos, G.Z. Kyzas, Agricultural peels for dye adsorption: a review of recent literature, J. Mol. Liq., 200 (2014) 381–389.
[5] J.A. Siles, F. Vargas, M.C. Gutiérrez, A.F. Chica, M.A. Martín, Integral valorisation of waste orange peel using combustion, biomethanisation and co-composting technologies, Bioresour. Technol., 211 (2016) 173–182.
[6] F. Girotto, L. Alibardi, R. Cossu, Food waste generation and industrial uses: a review, Waste Manage., 45 (2015) 32–41.
[7] X.M. Chen, A.R. Tait, D.D. Kitts, Flavonoid composition of orange peel and its association with antioxidant and anti-inflammatory activities, Food Chem., 218 (2017) 15–21.
[8] B. Ozturk, C. Parkinson, M. Gonzalez-Miquel, Extraction of polyphenolic antioxidants from orange peel waste using deep eutectic solvents, Sep. Purif. Technol., 206 (2018) 1–13.
[9] N. M'hiri, I. Ioannou, N. Mihoubi Boudhrioua, M. Ghoul, Effect of different operating conditions on the extraction of phenolic compounds in orange peel, Food Bioprod. Process., 96 (2015) 161–170.
[10] Z. Escobedo-Avellaneda, J. Gutiérrez-Uribe, A. Valdez-Fragoso, J.A. Torres, J. Welti-Chanes, Phytochemicals and antioxidant activity of juice, flavedo, albedo and comminuted orange, J. Funct. Foods, 6 (2014) 470–481.

[11] A.M. Torrado, S. Cortés, J.M. Salgado, B. Max, N. Rodríguez, B.P. Bibbins, A. Converti, J.M. Domínguez, Citric acid production from orange peel wastes by solid-state fermentation, Braz. J. Microbiol., 42 (2011) 394–409.
[12] B. Gómez, B. Gullón, C. Remoroza, H.A. Schols, J.C. Parajó, J.L. Alonso, Purification, Characterization, and prebiotic properties of pectic oligosaccharides from orange peel wastes, J. Agric. Food Chem., 62 (2014) 9769–9782.
[13] S. Lalou, F. Mantzouridou, A. Paraskevopoulou, B. Bugarski, S. Levic, V. Nedovic, Bioflavour production from orange peel hydrolysate using immobilized Saccharomyces cerevisiae, Appl. Microbiol. Biotechnol., 97 (2014) 9397–9407.
[14] G. Santi, S. Crognale, A. D'Annibale, M. Petruccioli, M. Ruzzi, R. Valentini, M. Moresi, Orange peel pretreatment in a novel lab-scale direct steam-injection apparatus for ethanol production, Biomass Bioenergy, 61 (2014) 146–156.
[15] N.R. Srinivas, Recent trends in preclinical drug–drug interaction studies of flavonoids—review of case studies, issues and perspectives, Phytother. Res., 29 (2015) 1679–1691.
[16] Z.Q. Zhang, J.J. Xiang, L.M. Zhou, Antioxidant activity of three components of wheat leaves: ferulic acid, flavonoids and ascorbic acid, J. Food Sci. Technol., 52 (2015) 7297–7304.
[17] A.V. Kurkina, Determination of total flavonoids in Siberian Hawthorn fruit, Pharm. Chem. J., 48 (2015) 800–803.
[18] R. Upadhyay, G. Nachiappan, H.N. Mishra, Ultrasound-assisted extraction of flavonoids and phenolic compounds from *Ocimum tenuiflorum* leaves, Food Sci. Biotechnol., 24 (2015) 1951–1958.
[19] V. Goulas, G.A. Manganaris, Exploring the phytochemical content and the antioxidant potential of Citrus fruits grown in Cyprus, Food Chem., 131 (2012) 39–47.
[20] M. Molina-Calle, F. Priego-Capote, M.D. Luque de Castro, Development and application of a quantitative method for determination of flavonoids in orange peel: influence of sample pretreatment on composition, Talanta, 144 (2015) 349–355.
[21] G.Z. Kyzas, D.N. Bikiaris, A.C. Mitropoulos, Chitosan adsorbents for dye removal: a review, Polym. Int., 66 (2017) 1800–1811.
[22] A. Khasri, M.R. Jamir, M.A. Ahmad, Adsorbent from orange peel for Remazol Brilliant dye removal: equilibrium and kinetic studies, AIP Conf. Proc., 2124 (2019) 020055.
[23] Y. Dai, Q. Sun, W. Wang, L. Lu, M. Liu, J. Li, S. Yang, Y. Sun, K. Zhang, J. Xu, W. Zheng, Z. Hu, Y. Yang, Y. Gao, Y. Chen, X. Zhang, F. Gao, Y. Zhang, Utilizations of agricultural waste as adsorbent for the removal of contaminants: a review, Chemosphere, 211 (2018) 235–253.
[24] A.G. Varghese, S.A. Paul, M.S. Latha, Remediation of heavy metals and dyes from wastewater using cellulose-based adsorbents, Environ. Chem. Lett., 17 (2019) 867–877.
[25] E. Joaquín-Medina, L. Patiño-Saldivar, A.N. Ardila-Arias, M. Salazar-Hernández, J.A. Hernández, Bioadsorption of methyl orange and methylene blue contained in water using as bioadsorbent Natural Brushite (nDCPD), Water Sci. Technol., 12 (2021) 304–347.
[26] S.H. Ranasinghe, A.N. Navaratne, N. Priyantha, Enhancement of adsorption characteristics of Cr(III) and Ni(II) by surface modification of jackfruit peel biosorbent, J. Environ. Chem. Eng., 6 (2018) 5670–5682.
[27] A.L. Arim, G. Guzzo, M.J. Quina, L.M. Gando-Ferreira, Single and binary sorption of Cr(III) and Ni(II) onto modified pine bark, Environ. Sci. Pollut. Res., 28 (2018) 28039–28049.
[28] A. Bhatnagar, M. Sillanpää, A. Witek-Krowiak, Agricultural waste peels as versatile biomass for water purification – a review, Chem. Eng. J., 270 (2015) 240–271.
[29] S.H. Peng, R. Wang, L.Z. Yang, L. He, X. He, X. Liu, Biosorption of copper, zinc, cadmium and chromium ions from aqueous solution by natural foxtail millet shell, Ecotoxicol. Environ. Saf., 165 (2018) 61–69.
[30] H.P. Chao, C.C. Chang, A. Nieva, Biosorption of heavy metals on Citrus maxima peel, passion fruit shell, and sugarcane bagasse in a fixed-bed column, J. Ind. Eng. Chem., 20 (2014) 3408–3414.
[31] M.R. Lasheen, N.S. Ammar, H. Ibrahim, Adsorption/desorption of Cd(II), Cu(II) and Pb(II) using chemically modified orange peel: equilibrium and kinetic studies, Solid State Sci., 14 (2011) 202–210.
[32] N.C. Feng, X.Y. Guo, Characterization of adsorptive capacity and mechanisms on adsorption of copper, lead and zinc by modified orange peel, Trans. Nonferrous Met. Soc. China, 22 (2012) 1224–1231.
[33] A. Chatterjee, S. Schiewer, Biosorption of cadmium(II) ions by citrus peels in a packed bed column: effect of process parameters and comparison of different breakthrough curve models, Clean–Soil Air Water, 39 (2011) 874–881.
[34] S. Elabbas, J.P. Leclerc, L. Mandi, F. Berrekhis, M.N. Pons, N. Ouazzani, Removal of Cr(III) from chrome tanning wastewater by adsorption using two natural carbonaceous materials: eggshell and powdered marble, J. Environ. Manage., 166 (2016) 589–595.
[35] J.V. Flores-Cano, R. Leyva-Ramos, F. Carrasco-Marin, A. Aragón-Piña, J.J. Salazar-Rabago, S. Leyva-Ramos, Adsorption mechanism of chromium(III) from water solution on bone char: effect of operating conditions, Adsorption, 22 (2016) 297–308.
[36] P.A. Kobielska, A.J. Howarth, O.K. Farha, S. Nayak, Metal–organic frameworks for heavy metal removal from water, Coord. Chem. Rev., 358 (2018) 92–107.
[37] D. Dias, N. Lapa, M. Bernardo, W. Ribeiro, I. Matos, I. Fonseca, F. Pinto, Cr(III) removal from synthetic and industrial wastewaters by using cogasification chars of rice waste streams, Bioresour. Technol., 266 (2018) 139–150.
[38] M. Ngabura, S.A. Hussain, W.A. Ghani, M.S. Jami, Y.P. Tan, Utilization of renewable durian peels for biosorption of zinc from wastewater, J. Environ. Chem. Eng., 6 (2018) 2528–2539.
[39] S. Guiza, Biosorption of heavy metal from aqueous waste solution using cellulosic orange peel, Ecol. Eng., 99 (2017) 134–140.
[40] D. Rathee, P. Rathee, S. Rathee, D. Rathee, Phytochemical screening and antimicrobial activity of *Picrorrhiza kurroa*, an Indian traditional plant used to treat chronic diarrhea, Arabian J. Chem., 9 (2016) S1307–S1313.
[41] S. Kiruba, M. Mahesh, Z.M. Paul, S. Jeeva, Preliminary phytochemical screening of the pericarp of *Crataeva magna* (Lour.) DC. – a medicinal tree, Asian-Pac. J. Trop. Biomed., 1 (2011) S129–S130.
[42] L. Liu, Y. Sun, T. Laura, X. Liang, Y. Hong, X. Zeng, Determination of polyphenolic content and antioxidant activity of kudingcha made from *Ilex kudingcha* C.J. Tseng, Food Chem., 112 (2009) 35–41.
[43] J.A. Hernández, F.A. Torres-García, M.M. Salazar-Hernández, R. Herrnández-Soto, Removal of chromium from contaminated liquid effluents using natural brushite obtained from bovine bone, Desal. Water Treat., 95 (2017) 262–273.
[44] R. Sudha, K. Srinivasan, P. Premkumar, Removal of nickel(II) from aqueous solution using *Citrus Limettioides* peel and seed carbon, Ecotoxicol. Environ. Saf., 117 (2015) 115–123.
[45] Y. Nogata, K. Sakamoto, H. Shiratsuchi, T. Ishii, M. Yano, H. Ohta, Flavonoid composition of fruit tissues of citrus species, Biosci. Biotechnol., Biochem., 70 (2006) 178–192.
[46] V. Lugo-Lugo, C. Barrera-Díaz, F. Ureña-Núñez, B. Bilyeu, I. Linares-Hernández, Biosorption of Cr(III) and Fe(III) in single and binary systems onto pretreated orange peel, J. Environ. Manage., 112 (2012) 120–127.
[47] C. Bertagnolli, M.G.C. da Silva, E. Guibal, Chromium biosorption using the residue of alginate extraction from *Sargassum filipendula*, Chem. Eng. J., 237 (2014) 362–371.
[48] B.E.L. Muñoz, R.R. Robles, J.L.I. García, M.T.O. Gutiérrez, Adsorption of basic chromium sulfate used in the tannery industries by calcined hydrotalcite, J. Mex. Chem. Soc., 55 (2011) 137–141.
[49] E.J. Kim, S. Park, H.J. Hong, Y.E. Choi, J.W. Yang, Biosorption of chromium (Cr(III)/Cr(VI)) on the residual microalga *Nannochloris oculata* after lipid extraction for biodiesel production, Bioresour. Technol., 102 (2011) 11155–11160.

[50] J.J. Jacob, R. Varalakshmi, S. Gargi, M.A. Jayasri, K. Suthindhiran, Removal of Cr(III) and Ni(II) from tannery effluent using calcium carbonate coated bacterial magnetosomes, Clean Water, 1 (2018) 1–10.
[51] M.E. Mahmoud, R.H.A. Mohamed, Biosorption and removal of Cr(VI)–Cr(III) from water by eco-friendly gelatin biosorbent, J. Environ. Chem. Eng., 2 (2014) 715–722.
[52] M.E.R. Carmona, M.A.P. da Silva, S.G.F. Leite, O.H.V. Echeverri, C. Ocampo-López, Packed bed redistribution system for Cr(III) and Cr(VI) biosorption by *Saccharomyces cerevisiae*, J. Taiwan Inst. Chem. Eng., 43 (2012) 428–432.
[53] V.K. Grupta, A. Nayak, Cadmium removal and recovery from prepared aqueous solutions by novel adsorbents from orange peel and Fe_2O_3 nanoparticles, Chem. Eng. J., 180 (2012) 81–90.
[54] K. Malook, I.U. Haque, Investigation of aqueous Cr(VI) adsorption characteristics of orange peels powder, Prot. Met. Phys. Chem. Surf., 55 (2019) 34–40.
[55] L. Sun, Y. Ma, H. Wang, T. Zhu, Synthesis of florisil materials modified with aliphatic or aromatic groups and the application for pipette-tip solid-phase extraction of rutin in orange peel, J. Sep. Sci., 41 (2018) 3716–3723.
[56] K. Pakshirajan, A.N. Worku, M.A. Acheampong, H.J. Lubberding, P.N. Lens, Cr(III) and Cr(VI) removal from aqueous solutions by cheaply available fruit waste and algal biomass, Appl. Biochem. Biotechnol., 170 (2013) 498–513.
[57] G. López-Téllez, C.E. Barrera-Díaz, P. Balderas-Hernández, G. Roa-Morales, B. Bilyeu, Removal of hexavalent chromium in aquatic solutions by iron nanoparticles embedded in orange peel pith, Chem. Eng. J., 173 (2011) 480–485.